Cystic fibrosis transmembrane conductance mutation detection using fluorescent hybridization probes and melting curves

Salah M. Bensaber[a], Ibrahim A. Marima[a], Anton Hermann[c], Abdul M. Gbaj[a,b]

[a]Department of Medicinal Chemistry, Faculty of Pharmacy, University of Tripoli, Tripoli, [b]Department of Genetics, National Medical Research Centre, Zawia, Libya, [c]Department of Cell Biology and Physiology, University of Salzburg, Salzburg, Austria

Correspondence to Abdul M. Gbaj, PhD, Department of Medicinal Chemistry, Faculty of Pharmacy, University of Tripoli, Tripoli, Postal Code M16, Libya Tels: +218 21 462 7798/218 21 462 8098; Fax: +218 21 462 5577; e-mail: abdulgbaj1@hotmail.com

Received 24 November 2016
Accepted 27 November 2016

Journal of The Arab Society for Medical Research 2016, 11:63–70

Background/aims
Single-point mutations or single-nucleotide polymorphisms, deletions, and insertions in genetic sciences are related to several human diseases, such as cancer, metabolic disorders, some types of mental illness, cardiovascular diseases, diabetes, etc. Consequently, precise, fast, and sensitive detection of these mutations in specific genes has substantial value in disease diagnosis, in the forecast of patients' responses to treatments, threat of deterioration of diseases, and outcomes. However, the existence of minute differences in structural and conformation dynamic stability from single base or multibase mismatches between the wild type (WT) and its mutated targets makes detection convenient. The common cause of cystic fibrosis (CF) is the deletion of three nucleotides (CTT). This deletion happens in the cystic fibrosis transmembrane conductance regulator (CFTR) gene, which involves the last cytosine (C) of isoleucine 507 (isoleucine 507ATC) and the two thymidine oligonucleotide (T) of phenylalanine 508 (phenylalanine 508TTT) codons. The significances of this important deletion are the deletion of phenylalanine at the 508 position of the cystic fibrosis transmembrane conductance regulator protein (ΔF508), an identical codon modification for isoleucine 507 (isoleucine 507ATT), and protein dysfunction.

Materials and methods
Fluorescence and ultraviolet–visible thermal studies were performed for WT and mutant-type target full systems. The target DNAs used were in the form of short oligonucleotides. The tandem probes system was used for detection of WT and single-nucleotide polymorphism alleles of human 3-bp ΔF508 (TTT) homozygous deletion. The pyrene dye attached to a probe oligonucleotide (15 mer) undergoes an excimer fluorescence intensity change on hybridization of the two probes to the WT compared with mutant-type targets.

Results
Our results indicate that the system consisting of the target sequence and the two probe oligonucleotides bearing the pyrene dye assemble correctly at the specified target. Once the full system (two probes and target) is arranged under suitable conditions, a red-shift emission and change in fluorescence intensity are seen at an excimer wavelength of 480 nm. Thermal studies also showed significant differences in T_m between mutated and unmutated CF genes. The results suggest that the differences in the fluorescence intensity at 480 nm and the spectrophotometric T_m (s) for the mutated and unmutated CF gene can be attributed to the type of binding of the probe to the target.

Conclusion
On the basis of the data obtained, we have chosen the probes possessing the highest fluorescence intensity along with the best deletion discrimination detection ability. The system was sensitive to deletion nucleotide polymorphisms and this may help in high-throughput applications in genetic testing and molecular diagnostics.

Keywords:
cystic fibrosis, deletions, excimer, fluorescence, single-nucleotide polymorphism

J Arab Soc Med Res 11:63–70

1687-4293

Introduction

Cystic fibrosis (CF) is a genetic disease that involves numerous organs such as the lungs, pancreas, liver, kidneys, and intestines. Patients with CF show many complications such as impenetrability in breathing and coughing up mucus due to frequent lung infections [1,2]. Other signs and symptoms in patients with CF comprise sinus microbial infections, abridged growth, fatty stool, deformity of the finger or toe, and male infertility. The degree of symptoms varies across individuals [1,2]. The average lifetime with CF is about 30 years. CF does not

 DOI: 10.4103/1687-4293.199297

follow an identical prototype in all patients but affects different people in different ways and at different degrees. However, the main problem occurs in the glands, which produce or secrete sweat and mucus. As is well known, sweat cools our body, and mucus lubricates the respiratory system, digestive system, and reproductive system, and stops tissues from drying and protects them from infections. People with CF lose extreme amounts of different salts when they sweat. This leads to upset equilibrium of minerals in the blood, which may lead to irregular heart rhythms. Shock is an important risk in CF patients. Mucus in CF patients is extremely thick and builds up in the intestines and lungs. The consequences are malnutrition, deprived growth, recurrent respiratory infections, breathing impenetrability, and finally enduring lung damage. Lung disease is the common cause of death in the majority of CF patients. CF can cause a variety of other medical problems such as sinusitis, nasal polyps, and clubbing. Other complications in CF patients are pneumothorax, hemoptysis, abdominal pain and discomfort, acidity, and rectal prolapse. Some people show manifestation of uncommon diseases, such as hepatic disease, diabetic mellitus, inflammation of the pancreas, and gallstones [3–5].

CF is a widespread autosomal recessive disorder found in people of Caucasian descent, like those of North America, Australasia, and Europe. CF is caused by genetic mutations and mainly deletions in the cystic fibrosis transmembrane conductance regulator (CFTR) gene. People with CF inherit the CFTR gene from both parents. Both genes are described as CFTR alleles. Although CF is a recessive disease, it will develop when deleterious mutations are found in both alleles of CFTR. When a harmful mutation is diagnosed on one allele of the CFTR, the individual will be known as a CF carrier. More than 2000 CF-causing CFTR mutations have been established. A CF patient could carry CFTR mutation on both CFTR alleles, or two dissimilar CF-causing CFTR mutations on both CFTR alleles [6–10]. CFTR is a membrane protein and consists of chloride channel in vertebrates that is translated by the CFTR gene [11–13]. The CFTR gene translates for a transporter that is an ABC transporter-class ion channel protein that transports chloride and thiocyanate ions [12] through epithelial cell membranes. The mutations of the CFTR gene have a significant influence on chloride ion channel function causing malfunction of epithelial fluid transport in the pancreas, lung, and other organs, leading to CF. Male infertility and congenital absence of the *vas deferens* are seen in male patients with CFTR, which result from the destruction and obstruction of the *vas deferens* and epididymis [14].

The gene that translates the human CFTR protein is found in chromosome seven. It is located on the long arm at position q31.2 [15,16]. Nearly 2000 mutations that cause CF have been listed [17–19]. ΔF508 is the most frequent mutation in CFTR, which results from deletion of three nucleotides and consequently leads to a loss of the amino acid phenylalanine at the 508th location on the protein. The consequence of this deletion is that the protein does not fold properly and is more easily degraded. There are other types of CF mutations but they are not common. The incidence of mutations is different across populations, and there is a need for genetic counseling and screening [18,20]. The CFTR gene is about 189 kb in length, with 27 exons and 26 introns [21,22]. CFTR is to some extent a long glycoprotein with 1480 amino acids. The CFTR protein is composed of five domains. There are two domains of transmembrane type; each of them contains six spans of alpha helices. These domains are connected to a nucleotide-binding domain, which is available in the cytoplasm. One of the binding domains is attached to the other domain by a dogmatic 'R' domain, which is a distinctive feature of CFTR. The channels of the ion can open only when phosphorylation of the R domain takes place by Protein kinase A (PKA) and ATP [23]. The COO^- terminal of the protein is attached to the cytoskeleton through a PDZ-interacting domain [24]. CFTR has a vital role as a gated ion that acts as an ATP-gated anion channel that increases the conductance for some important anions (e.g. chloride ion) to stream down their electrochemical current. ATP leads to structural changes in CFTR that open and close the ion gate to permit transmembrane stream of the anions downhill of their electrochemical gradient ability [13]. This is in contrast to the other ABC proteins, in which ATP leads to structural changes caused by uphill substrate transport through the biological cellular membranes. Fundamentally, CFTR is an ion channel that progresses as a busted ABC transporter type that trickles when in open structural conformation [13].

The frequency of CF has been studied in Europe. On average, one in 2000 to 3000 neonates are affected with CF. Still where populations are comparatively homogeneous, there might be noticeable local and regional dissimilarities. In France, for instance, there is a high occurrence of CF in northwest Brittany and a lower occurrence in the south [25,26]. CFTR gene mutations were extensively studied and published in European communities [25,26]. In many European countries, mutations have been extensively studied in more than 95% of the CFTR genes derived from CF patients. F508del CFTR mutation has been found to be the most frequent mutation causing CF. There is not a lot of information about CF occurrence in northern

African countries bordering the Mediterranean, even though small CFTR mutation detection studies have been performed in Libya, Tunisia, and Algeria, and they found the main mutations to be F508del, G542X, and N1303K [27–29].

The design of tools to detect point mutations [single-nucleotide polymorphism (SNP), one nucleotide insertion, or deletion] is a current challenge. Many techniques for genetic diagnostics have been developed in recent times [30]. A large part of these methods is based on hybridization of fluorescent oligonucleotide probe to its complementary DNA target to generate fluorescent signals. Pyrene conjugates of oligonucleotides as potential diagnostic probes have attracted the attention of researchers because of the unique properties of pyrene, such as long fluorescence lifetime, considerable sensitivity to the microenvironment, high quantum yield, and ability to form excimers and exciplexes [31,32].

Earlier, tandems of monopyrene-coupled oligonucleotides were designed for nucleic acid probing and SNP diagnostics [31,32]. The principle of action of these probes is based on the excimer formation at the tandem junction where a pyrene unit on the 3’-terminus of one component of the probe interacts with a pyrene unit on the 5’-terminus of another component. Tandem excimer probes are of particular interest in case of detection of such slight structural alterations caused by point mutations in DNA tandem complexes. In contrast to tandem probes relying on fluorescence resonance energy transfer [32] realized within 1–10 nm, excimer tandem probes rely on formation of excimer between two parallel pyrene units at a distance of only 3.4Å, which almost corresponds to the length of one base-pair along the DNA strand. We have been interested in designing a novel type of pyrene-coupled tandem as a point mutation probe possessing new qualities. 3’-pyrene and 5’-pyrene probes were chosen as a basis for these probes because of their numerous advantages including stability to endonucleases, high affinity to nucleic acids, and high rate of hybridization. The chosen probes are remarkable for their increased ability to discriminate mismatches in comparison with oligodeoxyribonucleotides.

Previously we have reported the construction of tandems of two pyrene-conjugated oligo as potential fluorescent SNP biosensors [33,34]. This study is targeted at the application of tandem probes relying on excimer formation between pyrene units at the tandem junction for detection of point mutations in the DNA target of CF by fluorescence emission and melting curve analysis with detection by ultraviolet (UV)–visible spectrum and excimer fluorescence changes.

Materials and methods

Materials and nature of the probes and targets

This study describes the experimental structures and conditions that permit strong excimer emission for nucleic acid detectors (Fig. 1), and shows how such excimers can detect the presence of deletions in CF. The excimer constructs used standard DNA base/sugar structures in both target and probes. The target was a part of the *Homo sapiens* CFTR, mRNA chromosome seven sequence (Genbank reference, NCBI Reference Sequence: NM_000492.3): 3′-TGGCACCATTA <u>AAGAAAATATCATCTTTGGTGTTTCCTATG</u> ATGAATATA-5′; the underline bases provided the complement to the target used. The ExciProbe probes had the sequences 5′-TTCTTTTATAGTAGA-3′-p and p-5′-AACCACAAAGGATAC-3′. The probes were supplied with a free 5′-phosphate group (p). DNA probes and DNA targets were obtained from Sigma-Proligo (Paris, France), and deuterium oxide was from Cambridge Isotope Laboratories (Goss-Scientific Instruments Ltd, Cambridge, UK). Distilled water was purified by ion exchange and charcoal using a MilliQ system (Millipore Ltd, Billerica, Massachusetts 01821, USA). Tris buffer was prepared from analytical reagent grade materials.

The pH values were measured using a Hanna Instruments (Hanna Company, UK) HI 9321 microprocessor pH meter, calibrated with standard buffers (Sigma-Aldrich, UK) at 20°C. High performance liquid chromatography was performed on an Agilent 1100 Series system (Agilent, USA), with both diode-array and fluorescence detection for online acquisition of spectra. Columns were Zorbax Eclipse X DB-C8 column (Zorbax, USA) (125 mm× 4.6 mm, 5 μm), or Luna C18 (2) (25 cm×4.6 mm, 5 μm), with an acetonitrile–water gradient from 0 to 50%.

Figure 1

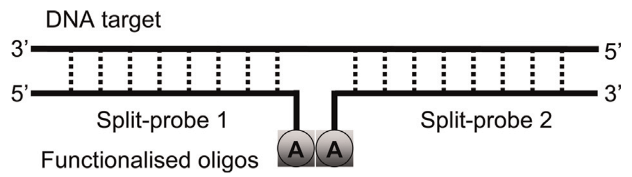

Synthetic target strands (50 mer) and nomenclature used for the excimer formation with wild type and mismatched targets. The excimers probes used were: 5′-TTCTTTTATAGTAGA-3′-pyrene (15 mer) and pyrene 5′-AACCACAAAGGATAC-3′ (15 mer). The dotted points are the three deleted oligonucleotide bases of cystic fibrosis.

Ultraviolet–visible spectrophotometry

UV-visible absorption spectra were measured at 20°C on a Peltier-thermostatted Cary-Varian 1E UV-visible spectrophotometer (USA). Quantification of oligonucleotide components used millimolar extinction coefficients (λ=260) of 178.6 for ExciProbe-3′-phosphate, 211.4 for ExciProbe-5′-phosphate, and 633.8 for 50-mer target. Extinction coefficients were calculated by the nearest neighbor method [35]; the contribution of the excipartners was small and could be neglected. T_m values (first derivative method) based on A_{260} were determined in Peltier-thermostatted quartz cuvettes using a Cary 4000 UV–visible spectrophotometer.

Melting temperature studies

Optical melting curves of the complexes were obtained using a Varian Cary 1E UV–visible spectrophotometer using a 1-ml optical cell with 1-cm path length. Tm measurements using the first derivative method, detected at 260 nm and accurate to around 0.1°C, were taken at 2.5 μmol/l component concentrations of the 1 : 1 : 1 complex in 80% Trifluoroethanol (TFE)/Tris buffer (10 mM Tris, pH 8.4, 100 mM NaCl). Melting data were also obtained from fluorescence emission spectra: the sample was heated to 60°C at a rate of 0.25°C/min. We used the wavelengths of λ_{ex} 340 nm and λ_{em} 376 nm for the pyrene monomer, and λ_{ex} 350 nm and λ_{em} 480 nm for the excimer. Recordings were made at 0.5°C increments. The sample was cooled at a rate of 0.13°C/min and the emission spectra were recorded once again. The melting curve obtained during cooling was used to determine T_m values.

Spectrophotofluorometry

Fluorescence emission and excitation spectra were recorded in four-sided quartz thermostatted cuvettes using a Peltier controlled-temperature Cary-Eclipse spectrofluorophotometer. All experiments were carried out at 5°C. 5′-pyrene was added first, followed by the 3′-pyrene probe and then the DNA target. Control experiments were conducted using 5′-pyrene first, followed by 3′-free oligonucleotides and then the target DNA. The mole ratio of oligonucleotide target DNA, 5′-probe and 3′-probe, was 1 : 1 : 1, and the concentration of each component was 2.5 μmol/l. Tris buffer was added at a concentration of 2.5 μmol/l either with or without 60% TFE, and the volume was adjusted to 100 μl with deionized water. Excitation wavelengths of 340 nm (for the pyrene monomer) and 350 nm (for the full split-probe system) were used at a slit width of 5 nm and recorded in the range of 350–650 nm. Emission spectra were recorded after each sequential addition of each component to record the change in emission due to each addition. A baseline spectrum of buffer, buffer plus water, and water plus 60% TFE was always carried out first. On each addition, the solution was left to equilibrate for ∼3–6 min in the fluorescence spectrophotometer, and emission spectra were recorded until no change in the spectra was seen to ensure that equilibrium had been reached.

Synthesis and oligonucleotide modification

Attachments of 1-pyrenemethylamine to oligonucleotide probes to 5′ and 3′ were as previously described [36].

Results

1-Pyrenemethylamine was conjugated to 3′ and 5′-oligonucleotide probes to give 3′-pyrene and 5′-pyrene attached probes. A characteristic purification chromatogram revealed that the free 3′-probe and 5′-probe oligonucleotides were eluted at a retention time of 18.9 min, trailed by 5′-pyrene–DNA conjugates at 22.1 min, 5′-bis-pyrene–DNA conjugate probes at 38 min, and lastly free, unconjugated 1-pyrenemethylamine at 40 min, with yields characteristically about 92%. The absorbance spectra of an unattached 5′-probe DNA and 3′-pyrene and 5′-pyrene–DNA probe confirmed the attachments. Additionally, the absorbance band at 348 nm is due to the attachments of pyrene, which as well changes the band at 260 nm. The proportion between the absorbance of the DNA at 260 nanometers (A=0.07) and 345 nanometers (A=0.037) was around 1.89, and attachments of 1-pyrenemethylamine to the 15-mer probe gave a ratio (A_{260}/A_{345}) of 3.1. The fluorescence emission spectra of the two pyrene attached probes have a highest emission at 380 nm, which corresponds to the presence of pyrene monomer fluorescence. The split-probe system using 3′-pyrene and 5′-pyrene in 60% TFE was used to recognize whether formation of excimer follows the same pattern published previously, in which they were using 3′-monopyrene and 5′-monopyrene DNA probes [36]. Experiments in this paper were performed with 60% TFE as an organic solvent to obtain a sharp excimer peak [36]. On addition of 50-mer synthetic DNA target, a characteristic broadband at 480 nm increases (Fig. 2); this massive change in the spectrum confirms the hybridization of the two probes to the 50-mer synthetic target. This is probably due to the interaction of the probes to the target forming an excimer, which has a massive emission at 480 nm compared with that of the pyrene monomer at 340 nm, which is actually a characteristic feature of the excimer formation between pyrene and pyrene.

Figure 2

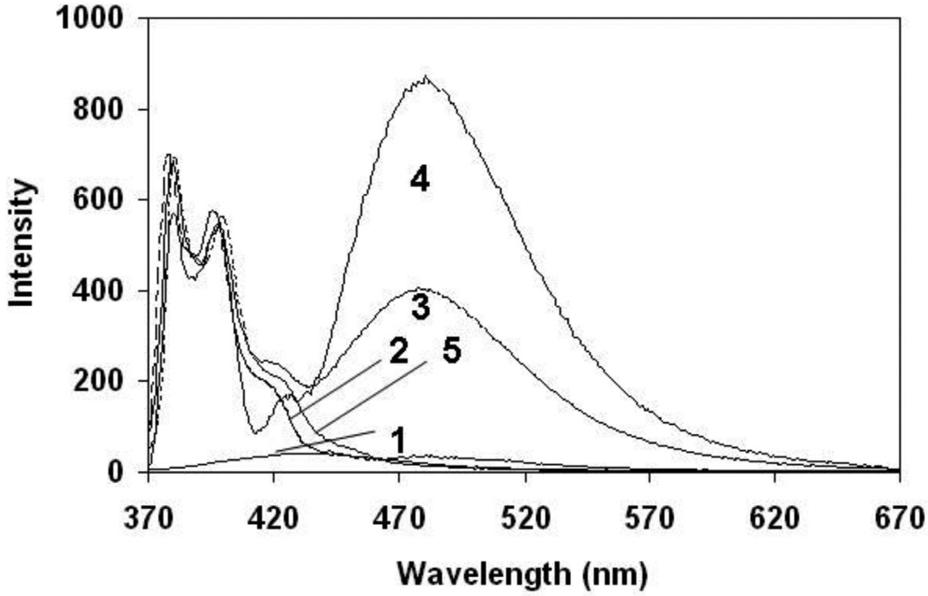

Fluorescence spectra of the split-DNA probe eximer system at 5°C. The spectra correspond to various stages of chronological self-assembly. **1:** [-5′-pyrene]; **2:** [-5′-pyrene+probe 3′Pyr]; **3:** full split-probe DNA system [3′pyrene+ –5′Pyr+Target 50 mer]; **4**: re-annealed system [3′-pyrene+-5′Pyr+DNA Target] after heating to 60°C and cooling back to 5°C. **5**: control DNA system [5′Pyr probe+Target] with unattached probe lacking the pyrene excipartner.

Figure 3

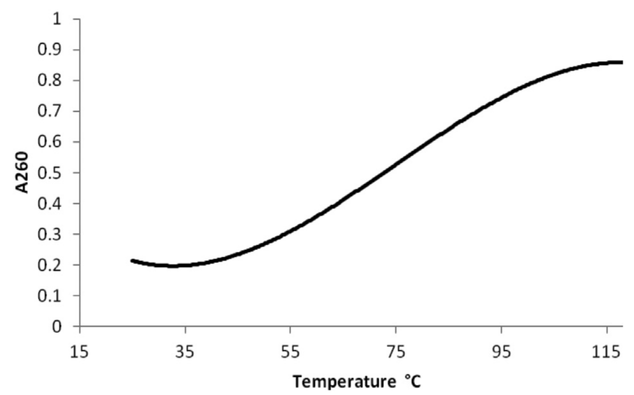

Melting curve of the cystic fibrosis target (full system: two 15-mer probes and 50-mer synthetic wild target) in 60% v/v trifluoroethanol/ Tris buffer (10 mM Tris, 0.1 NaCl, pH 8.4) illustrating the change in A_{260} (nm) as temperature was increased at 0.25°C/min.

Melting curve experiments

Melting temperature was calculated by using first derivative order methodology and the melting temperature of the full system in 60% v/v trifluoroethanol and Tris buffer (10 mM Tris, 0.1 M sodium chloride, pH 8.4). It was determined using UV-absorbance (A_{260}) and was found to be 82±2.01 °C (Fig. 3). The melting temperature is less than that found for the excimer probe system in water, which confirms that stabilization of the double-stranded DNA is no longer enhanced in the presence of 60% trifluoroethanol. Melting temperature of the normal CF target is 5.0°C higher than that of the mutated target. This difference in melting temperature is related to the fact that the normal DNA target with the two split probes is known to permit the stacking interactions and intercalation of the two split probes with the DNA target. These interactions between the probes and the target also stabilize the double-stranded DNA and therefore an enhancement in T_m would be seen in normal CF target in comparison with the mutated CF target.

Control experiments using 3′-phosphate oligonucleotide probe

To confirm whether the emission fluorescence arises from excimer formation among the required excimer pyrene partners (pyrene–pyrene excipartners) or with the nucleobases, control experiments were performed. The experiments were performed using 5′-pyrene–DNA attached probe, target and 3′-phosphate, DNA pyrene probe, and the 3′-probe holding only a phosphate group at its 'nick terminus', which demonstrated no excimer peak when bound to the complementary target (Fig. 2). This confirms that the second excipartner is required for excimer emission formation in the CF system.

Using 50-mer target containing three insertions of cystic fibrosis

A mutated CF target with three base-pairs between the two DNA probes was studied to verify whether similar changes in spectra can be obtained when no inserts are in attendance. The geometry, conformation, and distance between the two probes would alter the closeness of the pyrene molecules and consequently influence the interaction between the two pyrene molecules attached to the probes (Fig. 2).

Discussion

A large number of mutations causing CF were reported and studied extensively. To develop methods for genetic diagnosis and for homozygote and heterozygote screening, many scientific research groups used a lot of methods for competent analysis and understanding of the delta F508, G542X, G551D, R553X, and N1303K mutations [37,38]. They established that many mutations could be analyzed concurrently using hybridization with allele-specific oligonucleotide DNA probes. However, all of the CF mutations could be detected by DNA amplification followed by digestion restriction enzyme and then analysis of the PCR DNA products on polyacrylamide gels. At present, the most commonly used method is based on utilizing modified primers for DNA amplification to permit detection of any single-base change by restriction enzyme analysis. The common CF F508 mutation and three mutations in chromosomal exon 11 were fully studied using a multiplex amplification reaction, followed by enzyme double digestion with specific restriction enzymes. Finally, electrophoresis using polyacrylamide gel was performed [39]. The split-probe DNA system of the present paper uses synthetically externally oriented DNA-mounted excimer from two separate DNA probes planned to produce excimer emission by being precisely gathered *in situ* by hybridization with the complementary oligonucleotide target. In the CF case, a characteristic excimer fluorescence signal can be seen only after precise DNA double-strand formation of excimer-signal components with a DNA-matched target. In addition, this excimer signal at 480 nm will not be seen with unmatched targets. The benefit of the excimer-based split-probe approach is very low or zero background, specificity, and capability to detect DNA mismatches and insertions [40–42].

Data in this study (Fig. 2) revealed that the DNA probe bound to the synthetic target, which is commensurate with the reported literature [36]. Many studies have reported that the excimer fluorescence of the 3′ DNA probe and 5′ DNA pyrene attached probes is perceptive to their interactions with the matching strands as the 3′-pyrene and 5′-pyrene probes show a dramatic enhancement in the excimer fluorescence intensities on connecting precisely with the complementary targets. The developed 480 nm signal fluorescence of the 3′ DNA pyrene probe and 5′ DNA pyrene probe in the duplexes indicated that hybridization took place between pyrene residues on the specific target. Using a trifluoroethanol (60%) as an organic solvent allows the quantification of the target concentration as it effects on the excimer intensity in stoichiometric pattern. The advantage of the CF excimer system tested in this paper is the superior sensitivity system of a split-probe coordination.The spectrum pattern illustrated in this paper (Fig. 2) is reliable to that formerly reported for DNA pyrene probes [31,43–45]. The fluorescence changes in spectrum studied after addition of the 5′ DNA pyrene probe and 3′ DNA pyrene probe signify hybridization of the probe to the synthetic target. The presence of a large increase in pyrene–pyrene excimer signal at 480 nm and a decrease in pyrene monomer peak intensity confirms that the excimer formation is formed on hybridization of the probes to the target. This could be due to construction of the intramolecular structure of the pyrenes sandwich, which was extensively studied in the literature [46,47]. A standard experiment was performed to verify whether the emission develops from formation of excimer between the allocated DNA pyrene probes, or from the interaction between one of the pyrenes attached to the DNA probes and the nucleotide bases (A, T, C, G) of the CF gene sequence. The results obtained prove that the excimer emission obtained in this paper results from structural interaction between the two pyrene cystic fibrosis probes, and the interpretation that the excimer signals detected only in the presence of the full system on accurate hybridization of the DNA probe to the cystic fibrosis synthetic 50-mer-target strand and confirms the interaction of the excimer pyrene–pyrene rather than pyrene–DNA bases of the CF gene sequence.

A mutated CF 55-mer target with three deleted base-pairs between the two oligonucleotide probes was studied to determine whether similar changes in UV–visible and fluorescence spectra were noticed compared with the normal CF gene. The space between the two CF probes can influence the closeness of the pyrene-fluorescent molecules to each other and consequently influence the interaction between the two pyrenes. The excimer formation takes place only if the two CF probes are in close geometry (3–4 Å). If the two pyrene molecules are far away (100–1000 Å), the resultant fluorescence intensity signal is attributed to the fluorescence resonance energy transfer rather than excimer formation. The insertion of three base-pairs between the CF probes will create a distance longer than four angstrom, as the reported distance in the literature between each base-pair in DNA duplex arrangement is 3.4 Å [48]. A change in fluorescence intensity signal at 480 nm indicates that the increase in intensity was due to an interaction of the 3′-pyrene on the

DNA probe and the 5′-pyrene on the DNA probe, but only when they were in close proximity. Consequently, when the two probes attach to the CF target, the change in fluorescence intensity could be related to the excimer formation.

Insertions are anticipated to alter the proximity of the pyrene-fluorophores of the 3′ and 5′ DNA pyrene probes. Owing to the three oligonucleotide insertions, the DNA helical structures of the mutated CF target are expected to be different from that of wild type. These conformational changes would affect the three-dimensional orientation of the two pyrene molecules and significant changes in the fluorescence spectrum would be seen. Also, the insertions make the DNA structure less stable, and this leads to a massive drop in the excimer signal. These facts obtained in this paper express that the excimer probes system can recognize the CF insertions.

Hybridization of pyrene-CF probes to 50-mer DNA targets demonstrated that the 3′-pyrene and 5′-pyrene–DNA probes showed an increase in the fluorescence intensities of the excimer on precise arrangement of duplex with an unmutated target in a stoichiometric manner. Additionally, as the concentration of 50-mer CF target increases, the pyrene excimer peak at 480 nm reduces. In addition, the pyrene monomer peaks at 379 and 397 nm enhanced (data not shown), confirming that the ratio of monomer to excimer is influenced by the concentration of CF oligonucleotide target.

Conclusion

The present study established that DNA having a 3′ and 5′ DNA pyrene probe could be synthesized by phosphoramidate chemistry, purified, and quantified easily. The fluorescence excitation and emission spectra of the split-DNA probe system in 60% TFE indicate that the 5′ and 3′ DNA pyrene probes did not show any excimer emission intensity at 480 nm with synthetic CF DNA target with a three base-pair insertion. Moreover, CF insertions designated that it is probable for excimer systems to act as SNP detectors and might have the capability to identify SNP, which could be utilized for a variety of commercial and scientific purposes including evaluation of gene expression, medical diagnostics, drug discovery applications, genotyping, and gene delivery.

Financial support and sponsorship

Nil.

Conflicts of interest

There are no conflicts of interest.

References

1 Edmondson C, Davies JC. Current and future treatment options for cystic fibrosis lung disease: latest evidence and clinical implications. Ther Adv Chronic Dis 2016; 7:170–183.

2 Le MV, Gaillard JL, Herrmann JL. Vaccine strategies against bacterial pathogens in cystic fibrosis patients. Med Mal Infect 2016; 46:4–9.

3 Goldenberger D, Hinic V, Prince SS, Tamm M, Balestra AM, Hohler D, Frei R. A case report of a cystic fibrosis patient with repeated isolation of *Trichosporon mycotoxinivorans* identified by a novel short-extraction method. BMC Infect Dis 2016; 16:601–606.

4 Massie J. Breakthrough treatment in cystic fibrosis – Ivacaftor and sweat chloride. Pathology 2016; 48(Suppl 1):S15–S16.

5 Moran LP, Fischer S, Chouvarine P, Tummler B. Three-base periodicity of sites of sequence variation in *Pseudomonas aeruginosa* and *Staphylococcus aureus* core genomes. FEBS Lett 2016; 590:3538–3543.

6 Meng X, Clews J, Kargas V, Wang X, Ford RC. The cystic fibrosis transmembrane conductance regulator (CFTR) and its stability. Cell Mol Life Sci 2016; 73:1–16.

7 Schmidt BZ, Haaf JB, Leal T, Noel S. Cystic fibrosis transmembrane conductance regulator modulators in cystic fibrosis: current perspectives. Clin Pharmacol 2016; 8:127–140.

8 Carter SC, McKone EF. Pharmacogenetics of cystic fibrosis treatment. Pharmacogenomics 2016; 17:1453–1463.

9 Rosenfeld M, Sontag MK, Ren CL. Cystic fibrosis diagnosis and newborn screening. Pediatr Clin North Am 2016; 63:599–615.

10 Sosnay PR, Raraigh KS, Gibson RL. Molecular genetics of cystic fibrosis transmembrane conductance regulator: genotype and phenotype. Pediatr Clin North Am 2016; 63:585–598.

11 Jih KY, Hwang TC. Nonequilibrium gating of CFTR on an equilibrium theme. Physiology (Bethesda) 2012; 27:351–361.

12 Verkman AS, Galietta LJV. Chloride channels as drug targets. Nat Rev Drug Discov 2009; 8:153–171.

13 Gadsby DC, Vergani P, Csanady L. The ABC protein turned chloride channel whose failure causes cystic fibrosis. Nature 2006; 440: 477–483.

14 Marcorelles P, Gillet D, Friocourt G, Lede F, Samaison L, Huguen G, Ferec C. Cystic fibrosis transmembrane conductance regulator protein expression in the male excretory duct system during development. Hum Pathol 2012; 43:390–397.

15 Rommens JM, Iannuzzi MC, Kerem B, Drumm ML, Melmer G, Dean M, *et al.* Identification of the cystic fibrosis gene: chromosome walking and jumping. Science 1989; 245:1059–1065.

16 Frezal J, Baumann C, Kaplan J. Cystic fibrosis: a gene at the end of the road. Rev Prat 1990; 40:1543–1547.

17 Xu BP, Wang H, Zhao YH, Liu J, Yao Y, Feng XL, Shen KL. Molecular diagnosis of two Chinese cystic fibrosis children and literature review]. Zhonghua Er Ke Za Zhi 2016; 54:344–348.

18 Tsui LC, Dorfman R. The cystic fibrosis gene: a molecular genetic perspective. Cold Spring Harb Perspect Med 2013; 3:1–16.

19 Sosnay PR, Castellani C, Corey M, Dorfman R, Zielenski J, Karchin R, *et al.* Evaluation of the disease liability of CFTR variants. Methods Mol Biol 2011; 742:355–372.

20 Parisi GF, Cutello S, Di Dio G, Rotolo N, La Rosa M, Leonardi S. Phenotypic expression of the p.Leu1077Pro CFTR mutation in Sicilian cystic fibrosis patients. BMC Res Notes 2013; 6:461–466.

21 Lincke CR, Smit JJ, van d V, Borst P. Structure of the human MDR3 gene and physical mapping of the human MDR locus. J Biol Chem 1991; 266:5303–5310.

22 Tamburino L, Guglielmino A, Venti E, Chamayou S. Molecular analysis of mutations and polymorphisms in the CFTR gene in male infertility. Reprod Biomed Online 2008; 17:27–35.

23 Sheppard DN, Welsh MJ. Structure and function of the CFTR chloride channel. Physiol Rev 1999; 79 (Suppl):S23–S45.

24 Short DB, Trotter KW, Reczek D, Kreda SM, Bretscher A, Boucher RC, *et al.* An apical PDZ protein anchors the cystic fibrosis transmembrane conductance regulator to the cytoskeleton. J Biol Chem 1998; 273:19797–19801.

25 Ratbi I, Legendre M, Niel F, Martin J, Soufir JC, Izard V, *et al.* Detection of cystic fibrosis transmembrane conductance regulator (CFTR) gene rearrangements enriches the mutation spectrum in congenital bilateral absence of the vas deferens and impacts on genetic counselling. Hum Reprod 2007; 22:1285–1291.

26 Claustres M, Guittard C, Bozon D, Chevalier F, Verlingue C, Ferec C, *et al.* Spectrum of CFTR mutations in cystic fibrosis and in congenital absence of the vas deferens in France. Hum Mutat 2000; 16:143–156.

27 Hadj FS, Fattoum S, Chabchoub A, Messaoud T. First report of cystic fibrosis mutations in Libyan cystic fibrosis patients. Ann Hum Biol 2011; 38:561–563.

28 Loumi O, Ferec C, Mercier B, Creff J, Fercot B, Denine R, Grangaud JP. CFTR mutations in the Algerian population. J Cyst Fibros 2008; 7:54–59.

29 Estivill X, Bancells C, Ramos C. Geographic distribution and regional origin of 272 cystic fibrosis mutations in European populations. The Biomed CF Mutation Analysis Consortium. Hum Mutat 1997; 10:135–154.

30 Nakatani K. Chemistry challenges in SNP typing. Chembiochem 2004; 5:1623–1633.

31 Zhang Q, Deng T, Li J, Xu W, Shen G, Yu R. Cyclodextrin supramolecular inclusion-enhanced pyrene excimer switching for time-resolved fluorescence detection of biothiols in serum. Biosens Bioelectron 2015; 68:253–258.

32 Wu YX, Zhang XB, Li JB, Zhang CC, Liang H, Mao GJ, *et al.* Bispyrene-fluorescein hybrid based FRET cassette: a convenient platform toward ratiometric time-resolved probe for bioanalytical applications. Anal Chem 2014; 86:10389–10396.

33 Gbaj A, Bichenkova E, Walsh L, Savage H, Sardarian A, Etchells L, *et al.* New concepts of fluorescent probes for specific detection of DNA sequences: bis-modified oligonucleotides in excimer and exciplex detection. Libyan J Med 2009; 4:152–159.

34 Gbaj A, Walsh L, Rogert MC, Sardarian A, Bichenkova EV, Etchells LL, *et al.* Target-assembled exciplexes based on Scorpion oligonucleotides. Biosci Rep 2008; 28:1–5.

35 Weber G. Optimization method for obtaining nearest-neighbour DNA entropies and enthalpies directly from melting temperatures. Bioinformatics 2015; 31:871–877.

36 Bichenkova EV, Gbaj A, Walsh L, Savage HE, Rogert C, Sardarian AR, *et al.* Detection of nucleic acids in situ: novel oligonucleotide analogues for target-assembled DNA-mounted exciplexes. Org Biomol Chem 2007; 5: 1039–1051.

37 Marchand E, Verellen-Dumoulin C, Mairesse M, Delaunois L, Brancaleone P, Rahier JF, Vandenplas O. Frequency of cystic fibrosis transmembrane conductance regulator gene mutations and 5T allele in patients with allergic bronchopulmonary aspergillosis. Chest 2001; 119:762–767.

38 Endreffy E, Laszlo X, Szabo A, Roman F, Kurti K, Kalman M, Rasko I. Molecular genetic studies in monogenic and polygenic human diseases. Acta Biol Hung 1997; 48:121–128.

39 Ng IS, Pace R, Richard MV, Kobayashi K, Kerem B, Tsui LC, Beaudet AL. Methods for analysis of multiple cystic fibrosis mutations. Hum Genet 1991; 87:613–617.

40 Yguerabide J, Talavera E, Alvarez JM, Afkir M, Pyrene-labeled DNA. Probes for homogeneous detection of complementary DNA sequences: poly(C) model system. Anal Biochem 1996; 241:238–247.

41 Kumar P, Shaikh KI, Jorgensen AS, Kumar S, Nielsen P. Three pyrene-modified nucleotides: synthesis and effects in secondary nucleic acid structures. J Org Chem 2012; 77:9562–9573.

42 Bevilacqua PC, Li Y, Turner DH. Fluorescence-detected stopped flow with a pyrene labeled substrate reveals that guanosine facilitates docking of the 5' cleavage site into a high free energy binding mode in the Tetrahymena ribozyme. Biochemistry 1994; 33:11340–11348.

43 Reilly N, Ivanov M, Uhler B, Talipov M, Rathore R, Reid SA. First experimental evidence for the diverse requirements of excimer vs hole stabilization in Pi-stacked assemblies. J Phys Chem Lett 2016; 7:3042–3045.

44 Han G, Kim D, Park Y, Bouffard J, Kim Y. Excimers beyond pyrene: a far-red optical proximity reporter and its application to the label-free detection of DNA. Angew Chem Int Ed Engl 2015; 54: 3912–3916.

45 Zhou R, Xu C, Dong J, Wang G. Labeling-free fluorescent detection of DNA hybridization through FRET from pyrene excimer to DNA intercalator SYBR green I. Biosens Bioelectron 2015; 65:103–107.

46 Juskowiak B. Nucleic acid-based fluorescent probes and their analytical potential. Anal Bioanal Chem 2011; 399:3157–3176.

47 Fujimoto K. Highly emissive pyrene-based fluorophores and highly sensitive fluorescent sensors using pyrene emission switching. Yakugaku Zasshi 2010; 130:1283–1287.

48 Park H, Zhang K, Ren Y, Nadji S, Sinha N, Taylor JS, Kang C. Crystal structure of a DNA decamer containing a cis-syn thymine dimer. Proc Natl Acad Sci U S A 2002; 99:15965–15970.